ACADEMIC PRESS

Available online at www.sciencedirect.com
SCIENCE DIRECT®

Journal of Catalysis 215 (2003) 45–56

JOURNAL OF CATALYSIS

www.elsevier.com/locate/jcat

Aluminum-promoted tungstated zirconia catalyst in *n*-butane isomerization reaction

She-Tin Wong,[a] Tao Li,[a] Soofin Cheng,[a] Jyh-Fu Lee,[b] and Chung-Yuan Mou [a,c,*]

[a] *Department of Chemistry, National Taiwan University, Taipei 106, Taiwan, ROC*
[b] *Synchrotron Radiation Research Center, Hsinchu, Taiwan, ROC*
[c] *Center of Condensed Matter Science, National Taiwan University, Taipei 106, Taiwan, ROC*

Received 18 July 2002; revised 22 November 2002; accepted 26 November 2002

Abstract

The promotion effect of Al on tungstated zirconia (WZ) catalyst was studied in a butane isomerization reaction and compared with Fe-promoted catalyst (FWZ). XRD and EXAFS studies revealed an interaction between Al and WO_x, whereas XANES analysis indicates that the octahedral symmetry around W sites remained unchanged. Two Al^{3+} sites are present on co-precipitated Al-promoted WZ (AWZ_C) catalyst; one is formed by the substitution of Al species in the WO_x structure and the other is the terminal Al species anchoring on the WO_x surface. Only the terminal Al^{3+} sites are evident in impregnated AWZ catalyst. Our NH_3-TPD and DRIFT results suggest that these Al^{3+} sites are Lewis acid in nature with at least moderate acid strength. They are stronger than those Brönsted and Lewis acid sites originally present in WO_x. Exposure of the catalyst to atmospheric water results in the poisoning of these Al^{3+} sites by chemisorbed water, forming octahedral species. In an *n*-butane isomerization reaction, Al addition onto WZ increases both the activity and the stability of the catalysts. The catalytic activity of fresh catalysts decreases in the order $FWZ_I > AWZ_C \geqslant WZ_C$, whereas regenerated catalysts follow the order $AWZ_C \geqslant FWZ_I > WZ_C$. The improved activity of AWZ_C over WZ_C catalyst is related to the increased acidity created by the Al promoter. Most importantly, a great enhancement in catalytic activity was observed for regenerated catalyst relative to the fresh catalyst. The regenerated AWZ_C catalyst is as active as the FWZ_I catalyst.

Keywords: Tungstated zirconia; *n*-Butane isomerization; Promoter; Aluminum; Iron; Lewis acid site; Acid catalyst; EXAFS; NH_3-TPD; DRIFT

1. Introduction

Under the pressure of the world wide trend toward more severe environmental legislation and cleaner fuels, gasoline is reformulated by gradual replacement of aromatics with less hazardous components [1]. Isoalkanes may represent such a potential replacement, so that the high octane number of gasoline can be maintained. An important source of these high-octane isoalkanes is C_8 alkylates produced commercially by the alkylation of isobutane with butenes [2]. In this respect, skeletal isomerization of *n*-butane is an important reaction in petroleum chemistry and is usually performed with liquid superacids or Pt on chlorinated alumina. Isobutane is also the precursor for the synthesis of MTBE, ETBE, isoprenes, polyisobutene, *tert*-butyl alcohol, etc. Therefore, the interest in developing more efficient and cost-effective commercial processes for direct isomerization of *n*-butane and other light alkanes has increased in recent years.

The use of catalysts with strong acidity or superacidity is necessary to lower the reaction temperature of the acid-catalyzed skeletal isomerization reaction of *n*-butane since the thermodynamic equilibrium is in favor of isobutane only at low temperatures. However, the use of conventional catalysts results in serious environmental problems related to the recovery of corrosive acids and to the need for continuous supply of chlorinated compound to the reactants in the course of the reaction. Similar environmental concerns also arise regarding the use of sulfated zirconia (SZ), the solid superacid first discovered by Tanabe and Hattori [3]. Although high catalytic activity and product selectivity can be achieved in a skeletal isomerization reaction, serious concerns remain about the long-term sta-

* Corresponding author.
E-mail address: cymou@ms.cc.ntu.edu.tw (C.-Y. Mou).

0021-9517/03/$ – see front matter
doi:10.1016/S0021-9517(02)00176-8

bility of zirconia-supported sulfate species in reducing and oxidizing environments that are typical of hydrocarbon reactions and catalyst regeneration. There have been various efforts in adding promoters to stabilize the catalytic activities of SZ. The promotion effect of Al on a SZ system has been reported recently [4–6]. Al was found to retard the transformation of metastable tetragonal zirconia phase to monoclinic phase, helped to retain more sulfur on the catalyst surface, and also enhanced the number of acid sites with intermediate strengths. These two effects could be responsible for the significant enhancement of catalytic activity and stability of SZ catalysts after Al addition in a *n*-butane isomerization reaction at 250 °C.

As an alternative to SZ, tungstated zirconia (WZ) has become increasingly important since its discovery by Hino and Arata [7]. Later, it was demonstrated by several authors to be active in the isomerization of normal alkanes such as butane [8], pentane [9,10], and hexane [11,12]. The inorganic nature of this type of mixed oxide catalyst (WO_x/ZrO_2) ensures that they are stable in both oxidizing and reducing environments, even at high reaction temperatures. However, WZ is less active than SZ and promoters such as Pt and Fe have to be added. The former generates acid sites indirectly for the reaction [13], whereas the role of the latter is still a matter of speculation [14].

It is well-known that skeletal isomerization of *n*-butane occurs via a bimolecular mechanism involving a C_8 carbenium ion intermediate [15]. This intermediate was thought to be formed from the alkylation of a C_4 carbenium ion with butene. However, the mechanism of C–H bond breaking of *n*-butane, leading to the formation of a C_4 carbenium ion or butene on WZ, is still in dispute. WZ is generally accepted as merely a strong acid catalyst and not a superacid [16]. Hence, direct protolysis of *n*-butane is less likely to be the initial step of C–H bond activation. Recently, noncatalytic redox initiation processes have been proposed [17]. It is not surprising that most of the work on promoted WZ catalysts concentrated on transition metal promoters with redox behavior since transition metal oxides are widely used as alkane oxydehydrogenation catalysts. Our study, on the other hand, focuses on the importance of acidity in a *n*-butane isomerization reaction. Acid sites play the role of carbenium ion formation and we shall show that the addition of an acidic promoter such as Al can improve the catalytic performance of WZ catalysts.

In this paper, we study the promotion effect of Al and the acidic sites it generates directly on WZ catalysts. This study represents the first account of the promotion effect with a nontransition metal on WZ. The effect of Al addition on a WZ catalyst is discussed in Section 4.1. In Section 4.2, the performance of an AWZ catalyst is described. In Section 4.3, the nature and behaviour of acid sites in a catalytic reaction are proposed.

2. Experimental

2.1. Synthesis

WZ and Al-promoted WZ (AWZ) catalysts used in this study were derived from two separate sources. One series of WZ and AWZ catalysts were prepared by co-precipitation techniques adapted from the published procedures of Vartuli et al. [10], but zirconyl nitrate hydrate instead of zirconyl chloride octahydrate was used. The source of W is ammonium metatungstate hydrate, $(NH_4)_6W_{12}O_{39} \cdot xH_2O$, and Al promoter was introduced as $Al(NO_3)_3 \cdot 9H_2O$. The resulting mixture was adjusted to a pH of ~ 10 with concentrated NH_4OH and then subjected to hydrothermal reaction at 100 °C for 3 days. Only one Al loading was used, i.e., 1.0 wt%. Another series of catalysts was derived from commercially available WZ precursor (from MEL chemicals). AWZ catalysts with different Al content were prepared by an impregnation technique. For comparison purposes, Fe-promoted WZ (FWZ) was also prepared by impregnation of MEL WZ precursor with aqueous $Fe(NO_3)_3 \cdot 9H_2O$ solution. All the samples were calcined at 800 °C in static air for 3 h to form the mixed oxide. For the sake of clarity, the co-precipitated and impregnated catalysts are denoted by the subscripts C and I, respectively, in the title of the catalysts. Separate batches of these calcined materials were impregnated with the required amount of aqueous $PtCl_4$ solution and calcined at 500 °C in air for 3 h. They were denoted by the capital letter "P."

2.2. Characterization

The powder X-ray diffraction (XRD) patterns were recorded on nonoriented samples with a Scintag X1 diffractometer using Cu-K_α radiation (wavelength = 0.154 nm). BET surface areas were derived from N_2 adsorption data recorded at −196 °C on a Micromeritics ASAP 2000 apparatus. ^{27}Al magic angle spinning (MAS) NMR spectra were taken with a Bruker MSL 500 spectrometer using $AlCl_3$ solution as the external reference. Elemental composition (Pt, W, Fe, and Al) was analyzed with a simultaneous ICP-AES allied analytical system (Jarrel-Ash, Model ICAP 9000). Carbon analysis was done with a Heraeus VarioEL-III instrument.

Diffuse reflectance infrared Fourier-transformed (DRIFT) spectra were taken with a Bomem MB 100 FTIR spectrometer on powdered samples. For NH_3 adsorption experiments, the sample was first dehydrated in flowing dry N_2 at about 300 °C for nearly 2 h before introducing NH_3 at about 120 °C. The spectra were then recorded after about 15 min at each temperature, unless stated otherwise. They were presented as a Kubelka–Munk function using KBr as a reference [18].

Thermogravimetric analysis (TGA) was performed on a Du Pont 951 thermogravimetric analyzer with a heating rate of 10 °C/min under flowing dry air. The amount of NH_3

desorbed in the temperature-programmed desorption (NH_3-TPD) experiments was also determined by using the same Du Pont 951 thermogravimetric analyzer. The carrier gas and NH_3 were dried through molecular sieve and NaOH traps. The samples were dehydrated under flowing air at 500 °C for 1 h prior to NH_3 adsorption at 110 °C for 0.5 h. After the physisorbed NH_3 was removed by flushing with N_2 for 0.5 h, NH_3-TPD was started at a heating rate of 10 °C/min.

Studies on the W-L_{III}-edge X-ray absorption near-edge structure (XANES) and extended X-ray absorption fine structure (EXAFS) were performed at the Synchrotron Radiation Research Center (SRRC) in Hsinchu, Taiwan. The storage ring was operated at about 1.5 GeV with a ring current of about 200 mA. These experiments were done at room temperature in transmission mode with ionization detectors, and the data were collected twice for each sample to ensure reproducibility of results. The resulting EXAFS data were analyzed using the standard FEFF6 program. A detailed description of the data processing procedures can be found in the literature, e.g., Ref. [19]. The data were k^3-weighted to compensate for the attenuation of EXAFS amplitude at high k and then Fourier-transformed over the k-range of 2.0–11.5 A^{-1} with a Hanning apodization function of $dk = 2$ A^{-1}.

2.3. Catalysis

Catalytic study was carried out in a Pyrex microreactor flow system. The catalyst sample was mixed thoroughly with quartz sand and packed at the center of the reactor with a preheating zone of about 10 cm. Prior to reaction, the catalyst was pretreated at reaction temperature for about 2 h under a 10% H_2/N_2 gas mixture. The following reaction conditions were used for all catalytic runs: temperature, 300 °C; pressure, atmospheric; catalyst mass, 0.5 g; feed flow rate (at NTP), 6 ml min^{-1} of n-butane mixed with 12 ml min^{-1} of H_2. Reaction product was analyzed online by a Shimadzu GC-14B gas chromatograph, equipped with a FID and capillary column (DB-1, 60 m × 0.25 mm). Regeneration of used catalyst was carried out in situ under flowing air at 450 °C for 20 h, and reaction on regenerated catalyst followed the same conditions as the fresh catalyst.

Conversion of n-butane is defined as the percentage of n-butane converted to hydrocarbon products, whereas isobutane selectivity is the percentage of isobutane in the observed product. These data were based on carbon number. In most cases, the activity of catalyst was expressed in term of turnover frequency (TON), which is the amount of n-butane (in μmol) converted per second per gram of catalyst. Conversion values of n-butane can be converted to TON using the reaction parameters outlined above.

3. Results

3.1. Composition of catalysts

The co-precipitated catalysts contained about 14–15 wt% of W metal, which is slightly higher than those from MEL (11–14 wt%). These loadings are not far from the theoretical monolayer capacity of 7.3 W atoms nm^{-2}, which is equivalent to about 12–13 wt% of W [13]. The Pt content was between 0.4 and 0.5 wt% for all Pt-loaded catalysts. In FWZ_I catalyst, the Fe content was 1.2 wt%. The Pt and Fe loadings were chosen to give the optimum performance of the catalyst. We have found that the catalytic activity of 1.2 wt% FWZ_I sample gave much higher activity than 0.3 wt% sample, whereas in the SZ system, a 0.2 wt% sample gave maximum activity [20]. The content of Al in AWZ catalysts will be described separately in the text.

All the freshly prepared WZ catalysts are yellowish in color. In the impregnated AWZ catalyst, the sample color turns white upon the introduction of only 0.6 wt% Al. In the co-precipitated AWZ catalyst, however, the sample color is not homogeneously white, even after the addition of 1.0 wt% Al. This sample contains a mixture of yellowish and white particles.

3.2. XRD study

Figs. 1a and 1b show the XRD patterns of WZ and AWZ catalysts prepared by impregnation and co-precipitation methods, respectively. The assignment of peaks was made according to the literature [11,21,22]. All these samples contain zirconia primarily in the tetragonal phase. Only a minute amount of monoclinic phase zirconia is present on WZ and the addition of Al decreases it further.

The effect of Al on the peak intensity of tetragonal phase WO_3 ($2\theta = 23$–$25°$) is different in impregnated and co-precipitated AWZ catalysts. In the case of co-precipitated samples, the relative intensity of WO_3 peaks is only slightly affected after the addition of 1.0 wt% Al on WZ. Also, the group of small peaks between $2\theta = 50°$ and $2\theta = 60°$ belonging to the same WO_3 phase becomes less obvious after Al addition. In the case of impregnated sample, the addition of only 0.6 wt% Al on WZ causes the complete disappearance of WO_3 peaks.

3.3. Surface area measurements

The BET surface areas of the promoted and nonpromoted WZ catalysts are comparable to the literature-reported values [10,23]. For co-precipitated WZ and AWZ catalysts, the surface areas are 78 and 65 $m^2\,g^{-1}$, respectively. The surface area, at 70 to 80 $m^2\,g^{-1}$, for a series of impregnated AWZ catalysts is listed in Table 1. A slight increase in surface area can be seen only for the sample at high Al content.

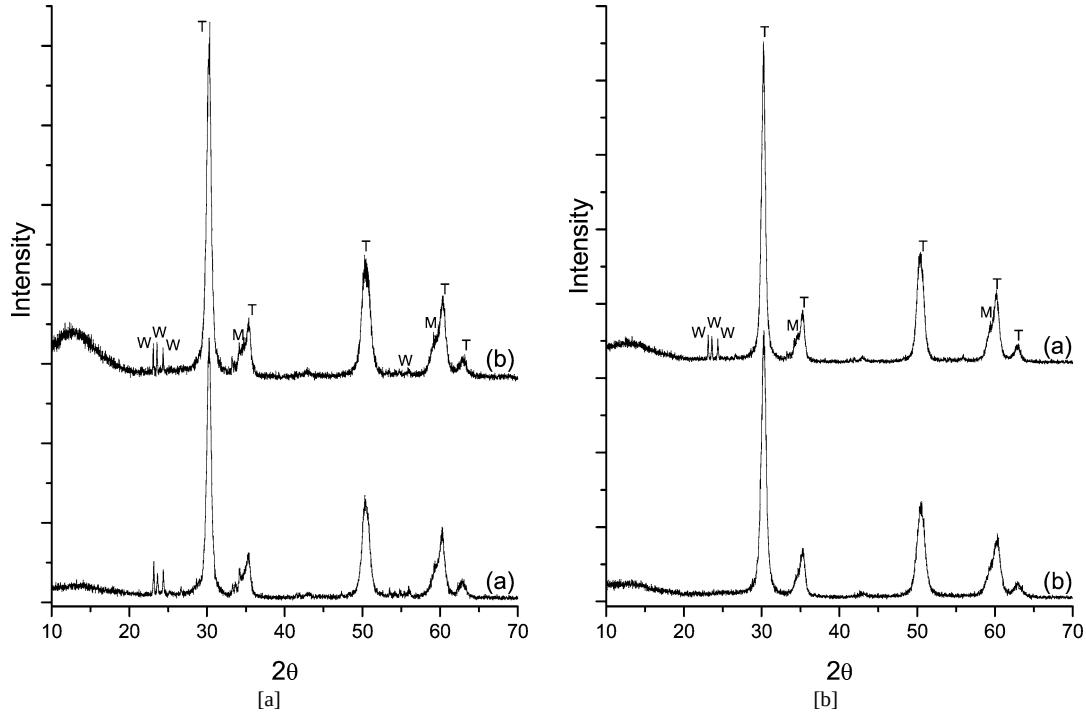

Fig. 1. [a] XRD patterns of catalysts prepared by the co-precipitation method: (a) WZ and (b) 1.0 wt% AWZ. T = tetragonal zirconia, M = monoclinic zirconia, and W = tetragonal WO_3. [b] XRD patterns of catalysts prepared by the impregnation method: (a) WZ and (b) 0.6 wt% AWZ. Peak assignments are similar to those in Fig. 1a.

Table 1
Effect of Al content on the catalytic performance and surface area of WZ catalysts

Al content (wt%)	TON[a] (μmol g^{-1} s^{-1})		Selectivity[b] (%)		Surface area (m^2 g^{-1})
	Initial	Final	Initial	Final	
0	0.16	0.08	88.9	90.6	68
0.6	0.54	0.25	89.6	90.5	75
1.2	0.49	0.22	89.3	89.7	69
2.3	0.15	0.07	86.5	87.9	81

[a] Data taken from regenerated catalysts. Initial and final data were obtained after 5 min and 6 h on stream, respectively.

[b] Selectivity to isobutane.

3.4. ^{27}Al MAS NMR study

The ^{27}Al MAS NMR spectra of AWZ catalysts prepared from both co-precipitation and impregnation methods are presented in Fig. 2. From the value of chemical shift (ppm), the coordination symmetry around Al sites can be predicted.

The spectra of all the AWZ catalysts consist of only a strong resonance between −0.824 and −0.536 ppm, which is very close to the value for the external standard ($AlCl_3$ solution, 0 ppm). Hence, we assigned this resonance to Al in octahedral sites. In addition, we have found that this resonance signal is broader in impregnated AWZ catalysts than co-precipitated catalyst. This shows that the chemical environment of the octahedral Al species in the co-precipitated catalyst is more uniform. The broad resonance centered at around 30 ppm in these spectra can be due to Al species in a disordered state.

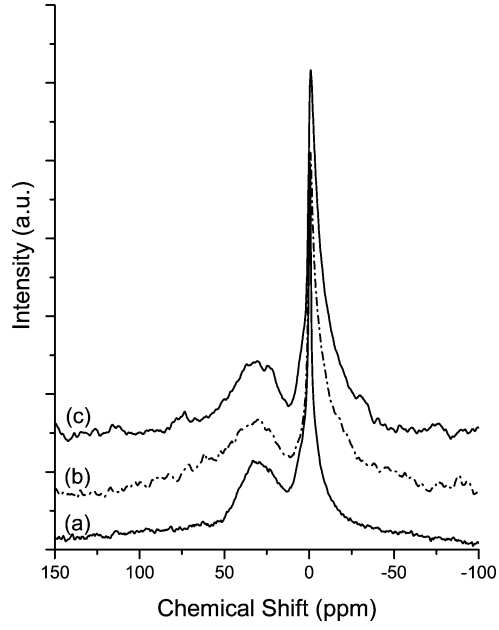

Fig. 2. ^{27}Al MAS NMR spectra of AWZ catalysts prepared by (a) co-precipitation, 1.0 wt% Al; (b) impregnation, 0.6 wt% Al; and (c) impregnation, 1.2 wt% Al.

3.5. TGA study

To understand why the fresh and regenerated catalysts can give rise to different catalytic performance, we compare the amount of residual chemisorbed water present on both catalytic states prior to the reaction. It should be mentioned

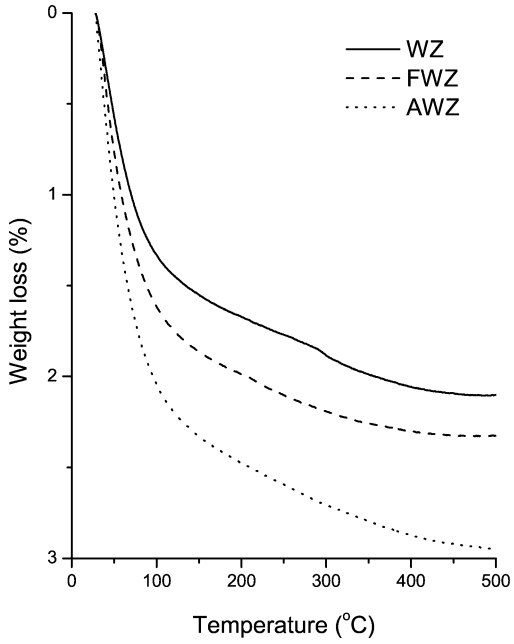

Fig. 3. Dehydration profiles of fresh WZ_C, AWZ_C, and FWZ_I catalysts.

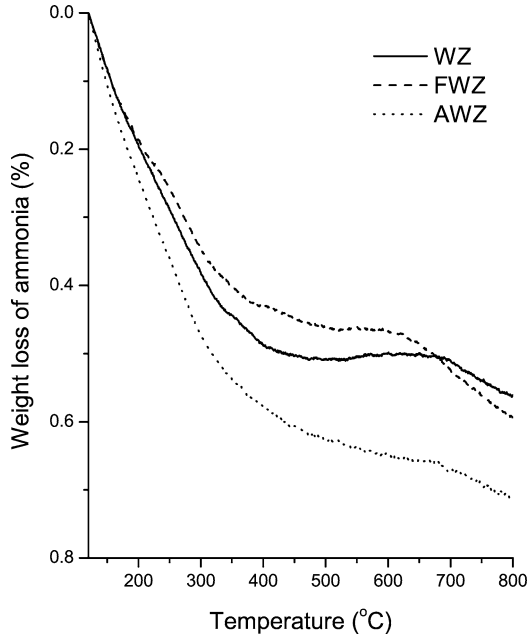

Fig. 4. NH_3-TPD profiles of fresh WZ_C, AWZ_C, and FWZ_I catalysts.

again that the regenerated catalyst has undergone treatment at 450 °C whereas fresh catalyst was pretreated only at 300 °C. Fig. 3 shows the weight loss profiles of co-precipitated WZ and AWZ catalysts together with the reference FWZ_I catalyst in the dehydration study under flowing air. These catalysts have been long exposed to air. The use of air as the carrier gas minimized the loss of WO_x lattice oxygen. Obviously, AWZ_C catalyst adsorbed the most water than the other two catalysts. One can also see that all the catalysts have less chemisorbed water in the regenerated state (450 °C) than the fresh state (300 °C). Specifically, AWZ_C catalyst loses more water than FWZ_I in going from a fresh to a regenerated state (0.22 versus 0.13 wt%). On the other hand, WZ_C has a comparable amount of water loss (0.21 wt%) to AWZ_C in the same process.

3.6. NH_3-TPD study

To understand the promotion effect of Al, we used the NH_3-TPD technique to compare the acidic characteristics of the same set of WZ, AWZ, and FWZ catalysts described in Section 3.5. Fig. 4 shows the NH_3-TPD profiles of these catalysts without Pt addition. Total acidity was calculated from the weight loss of NH_3 between 150 and 600 °C and the magnitudes are 0.54, 0.42, and 0.38 wt% for AWZ_C, WZ_C, and FWZ_I catalysts, respectively. The large drop in catalyst weight beyond 600 °C is probably due to the loss of lattice oxygen from WO_x since a blank study on WZ_C without NH_3 adsorption gave similar weight loss at temperatures $\geqslant 600$ °C.

It is obvious that AWZ_C catalyst has the highest total acidity, judging from the weight loss of NH_3 between 150 and 600 °C. This result shows clearly that the addition of Al caused an increase in total acidity of WZ_C catalyst. Moreover, the NH_3 weight loss in AWZ_C catalyst continued between 400 and 625 °C but it levels off for WZ_C catalyst. It seems that a new type of acid sites is generated by aluminum addition, and these sites are stronger acids. We have also carried out NH_3-TPD experiments for aluminosilicate materials such as H-mordenite and found a steep weight loss in a similar temperature range (325–500 °C). Interestingly, our reference FWZ_I catalyst has lower total acidity than WZ_C catalyst.

3.7. DRIFT study

The study on NH_3 adsorption by DRIFT has been commonly employed to evaluate the surface acidity of a catalyst. In this study, the same technique was used to compare the acidity of WZ and AWZ catalysts. Two types of acid sites were found on both catalysts, namely, the Brönsted sites (B) and Lewis sites (L). The assignment of infrared bands was made according to the published work of Baertsch et al. [24].

Fig. 5 compares the DRIFT spectra of co-precipitated WZ catalyst before and after NH_3 adsorption at 250 °C. Upon the adsorption of NH_3, one can see that the broad band due to stretching vibrations of Zr–OH and W–OH groups diminished with the simultaneous generation of a more intense broad band at a lower frequency of 2500–3600 cm^{-1}. The latter is due to a combination of N–H stretching vibrations of hydrogen-bonded NH_3, as well as the shift in O–H stretching vibrations to lower frequency as a result of hydrogen bonding with adsorbed NH_3. In addition, the band due to the stretching mode of W=O functional group at the surface of WZ can be observed at 2017 cm^{-1}.

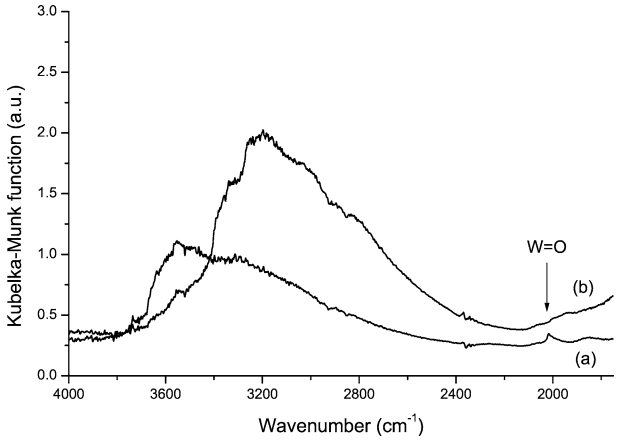

Fig. 5. DRIFT spectra of co-precipitated WZ catalyst at 250 °C: (a) before NH_3 adsorption and (b) after NH_3 adsorption.

The DRIFT spectra of co-precipitated WZ and AWZ catalysts after NH_3 adsorption and desorption at different temperatures are given in Figs. 6a and 6b, respectively.

In the case of WZ_C catalyst, the intense band at 1417 cm^{-1} (δ_{as}, denoted as B_L) and a small shoulder at about 1656 cm^{-1} (δ_s, denoted as B_H) correspond to NH_4^+ on Brönsted acid sites. The bands due to NH_3 coordinated to Lewis acid sites, however, appear at 1606 cm^{-1} (δ_{as}, denoted as L_H) with a weak shoulder at 1271 cm^{-1} (δ_s, denoted as L_L). Here, one should take notice that the subscripts L and H following the symbols of acid sites (B and L) represent low- and high-frequency bands, respectively. All the bands decrease in intensity with increasing desorption temperatures, indicating the loss of NH_3 adsorbed on Brönsted and Lewis acid sites. However, it seems that Brönsted acid sites here are stronger than Lewis acid sites since they still retain a significant amount of NH_3 at 400 °C, whereas the NH_3 adsorbed on Lewis acid sites is almost completely removed. Also, the B_L band shifts slightly to lower frequency as the desorption temperature increases. This phenomenon happens for all catalysts with a shift between 4 and 13 cm^{-1}. After prolonged heating (e.g., 3 h) at 450 °C, B_H, B_L, and L_H bands disappeared altogether, whereas the L_L band disappeared after heating at a lower temperature of 400 °C.

In the case of AWZ_C catalyst, the spectral features are somewhat different from those of the WZ_C catalyst. Qualitatively, we find that the intensity of all bands decreased in intensity. The frequency of the B_H, B_L, and L_H bands are consistent with those of the WZ_C catalyst. However, a new L_L (L_{LN}) band now appeared at 1287 cm^{-1}. As the desorption temperature of NH_3 increases, its frequency shifts gradually to a higher value and reaches 1302 cm^{-1} at 450 °C. The frequency of this symmetric N–H deformation mode appears to correlate directly with the Lewis acid strength of the coordinating cation [24]. The observed shift to higher frequency with the increase in desorption temperature indicates an increased acid strength at higher desorption temperatures. Most importantly, this band remained prominent, even after the sample was subjected to a

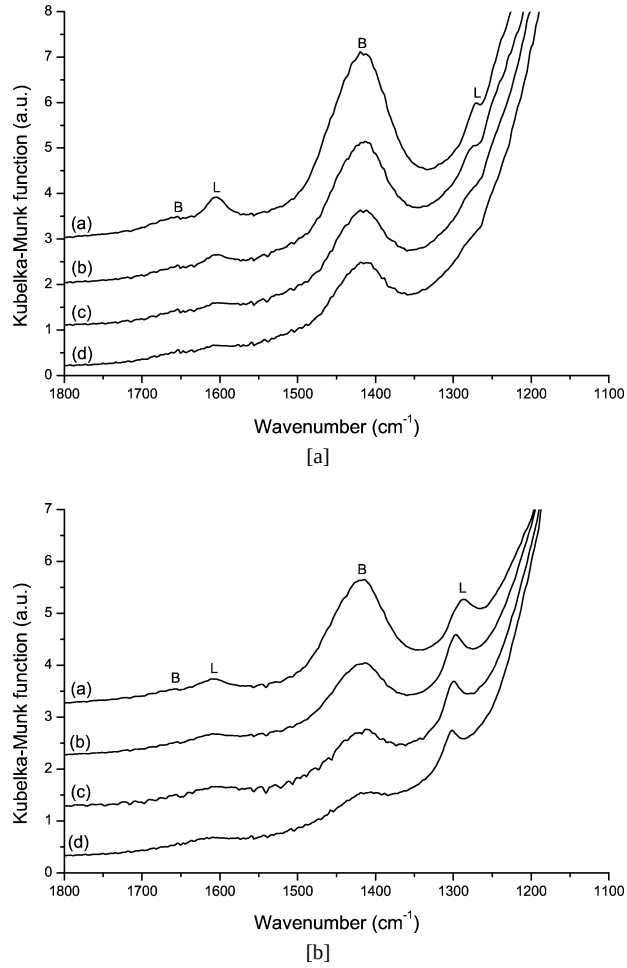

Fig. 6. [a] DRIFT spectra of NH_3-adsorbed co-precipitated WZ catalyst after desorption at (a) 250 °C, (b) 350 °C, (c) 400 °C, 15 min, and (d) 400 °C, 45 min. B = Brönsted acid sites and L = Lewis acid sites. [b] DRIFT spectra of NH_3-adsorbed co-precipitated AWZ catalyst after desorption at (a) 250 °C, (b) 350 °C, (c) 400 °C, and (d) 450 °C. Band assignments are similar to those in Fig. 6a.

high-temperature treatment of 450 °C. Obviously, this L_{LN} band in the AWZ_C catalyst corresponds to a new type of Lewis acid sites that is different from those in the WZ_C catalyst with a band at 1271 cm^{-1}. Its acid strength is stronger than that of all the acid sites previously observed on WZ_C catalysts. After the catalyst was regenerated by heating at 450 °C for 3 h followed by readsorption of NH_3, all the peaks due to NH_3 adsorption on B and L sites can be recovered (figure not shown).

The DRIFT spectra of impregnated WZ and AWZ catalysts with NH_3 adsorption–desorption at different temperatures are shown in Figs. 7a and 7b, respectively. Generally, the spectral features of these catalysts are similar to those of the corresponding co-precipitated catalysts except that its bands are less intense. However, small variations in spectral features are still observed.

In WZ_I catalyst, the frequency of the B_H, B_L, and L_H bands are also consistent with those of the co-precipitated WZ catalyst. Interestingly, two L_L bands now appeared

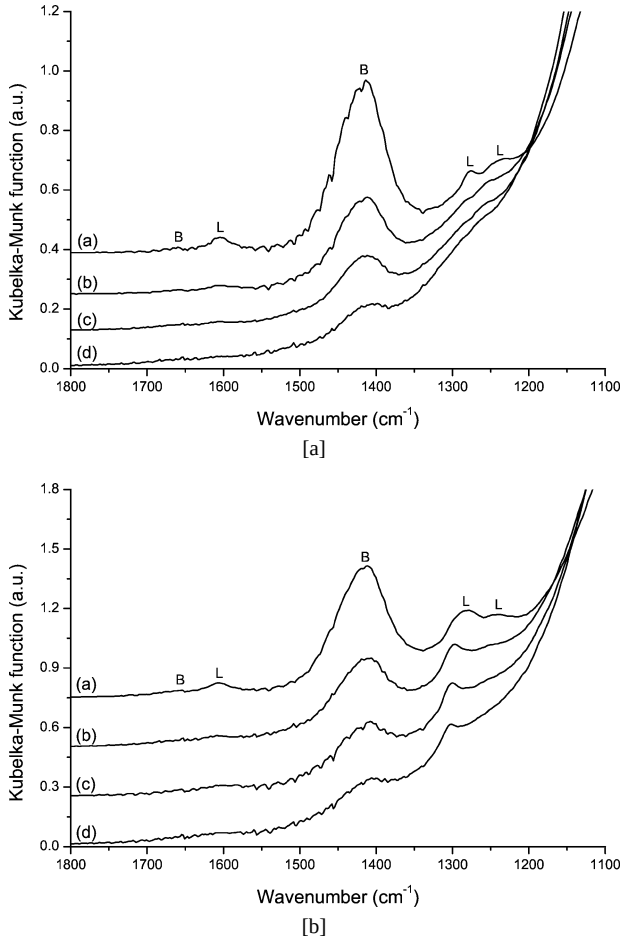

Fig. 7. [a] DRIFT spectra of NH_3-adsorbed impregnated WZ catalyst after desorption at (a) 250 °C, (b) 350 °C, (c) 400 °C, and (d) 450 °C. Band assignments are similar to those in Fig. 6a. [b] DRIFT spectra of NH_3-adsorbed impregnated AWZ catalyst after desorption at (a) 250 °C, (b) 350 °C, (c) 400 °C, and (d) 450 °C. Band assignments are similar to those in Fig. 6a.

at 1276 and ∼1237 cm^{-1}. The latter is denoted here as $L_{L'}$. The L_L band (1276 cm^{-1}) is similar in nature to that observed in the co-precipitated catalyst. However, the natures of both these Lewis acid sites are not examined in detail.

In the AWZ_I catalyst, the frequency of the B_H, B_L, and L_H bands are also consistent with those of the co-precipitated WZ catalyst. In addition, the L_{LN} band previously described in co-precipitated AWZ catalyst is also observed here. Its frequency also shifted from 1282 to 1302 cm^{-1} at 450 °C. Of course, the $L_{L'}$ band also appeared at ∼1239 cm^{-1}. After the catalyst was regenerated by heating at 450 °C for 3 h followed by re-adsorption of NH_3, all the bands due to NH_3 adsorption on B and L sites can be recovered (figure not shown).

3.8. XANES and EXAFS studies

The W-L_{III}-edge XANES spectra of WZ and AWZ catalysts were also recorded at room temperature without any dehydration pretreatment (figure not shown). Similar spectral features were observed in the catalysts prepared by impregnation and co-precipitation methods. The shape and fwhm of the "white line" in the W-L_{III}-edge portray distinctions between tetrahedral and octahedral tungsten oxides [25]. The broad white line in the spectra of all our WZ and AWZ catalysts has a fwhm of ∼9 eV. Most importantly, Al addition on WZ does not alter its spectral features.

Figs. 8a and 8b show the Fourier-transformed W-L_{III}-edge EXAFS radial distribution function (RDF) of WZ and AWZ catalysts prepared by co-precipitation and impregnation methods, respectively. These RDFs are not corrected for phase shifts. The assignment of peaks was made according to the published work of Hilbrig et al. [25] on titania- and alumina-supported tungsten oxide system. Generally, the RDFs of WZ_C and WZ_I are similar to that of bulk WO_3. The peaks between $R = 0.6$ and $R = 2.0$ Å in the RDF plots are due to W–O bond distances but only the strongest one is labeled for simplicity. We note that the W–O–W bond distance of WZ_C and WZ_I is about 0.31–0.37 Å less than that of bulk WO_3, indicating that it is sensitive to the support. The peak at a slightly shorter bond distance than W–O–W cannot be assigned without ambiguity. Unlike bulk WO_3 and WZ_I, its intensity is higher than that of the W–O–W peak in WZ_C. This phenomenon probably reveals a greater contribution of W–O–Zr linkage to the intensity of this peak in WZ_C than in WZ_I. We thus tentatively assigned this peak to mixed scatterers, i.e., W–O–W/Zr. However, one should note that if aluminum is substituted in the WO_x structure, it could also contribute to this peak since its position in the structure may not be exactly symmetrical.

The new peaks appeared in the RDF plots of AWZ and not found in WZ catalyst are assigned to W–O–Al distances. There is only one W–O–Al distance in both of the impregnated AWZ catalysts (3.90–3.96 Å), but two W–O–Al distances are observed in the co-precipitated catalyst (3.44 and 3.87 Å). In addition, we note that the addition of Al causes the W–O–W distance to shrink slightly (from 3.25 to 3.19 Å) in the impregnated sample, but more significantly (from 3.19 to 3.07 Å) in the co-precipitated sample. The main W–O distance of the impregnated sample also varies from 1.26 Å in WZ to 1.32 Å (1.2 wt%) and 1.29 Å (2.3 wt%) in AWZ, whereas it remained unchanged in the co-precipitated sample at 1.29 Å (1.0 wt%), even after considerable broadening due to overlapping of other W–O peaks.

3.9. Catalysis

Under our reaction conditions, the main product in *n*-butane isomerization reaction was isobutane with at least 86% selectivity (carbon basis) and getting higher if Pt is present. Minor products were methane, ethane, propane, *n*-pentane, and isopentane.

For the catalytic study on the promotion effect of Al on WZ catalyst, commercially available WZ precursor (MEL)

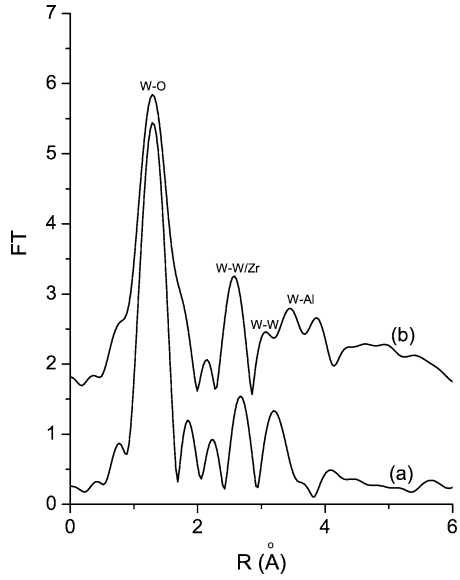

[a]

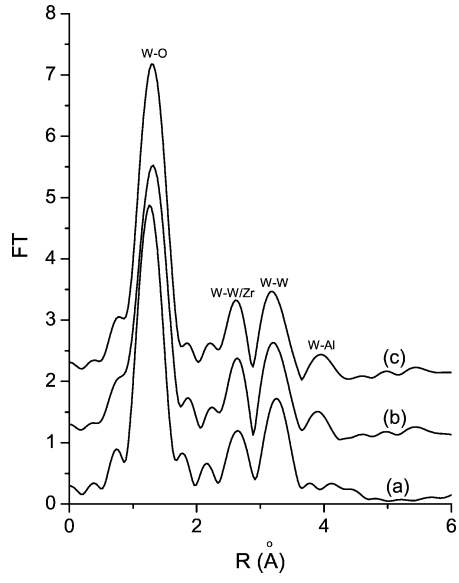

[b]

Fig. 8. [a] W-L_{III}-edge EXAFS radial distribution functions of co-precipitated catalysts: (a) WZ and (b) 1.0 wt% AWZ. The oxygen atom between two metal atoms is omitted for clarity. [b] W-L_{III}-edge EXAFS radial distribution functions of impregnated catalysts: (a) WZ, (b) 1.2 wt% AWZ, and (c) 2.3 wt% AWZ. The oxygen atom between two metal atoms is omitted for clarity.

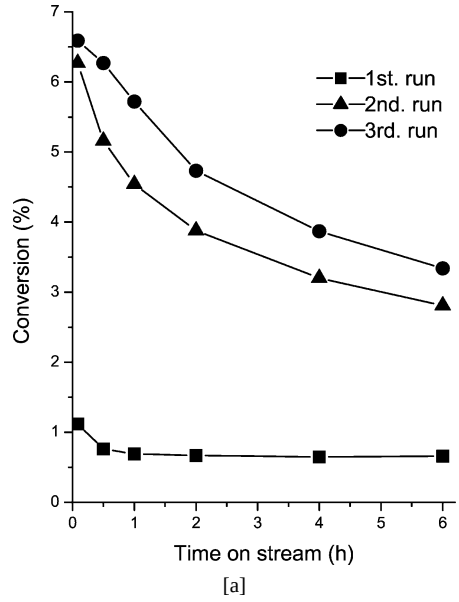

[a]

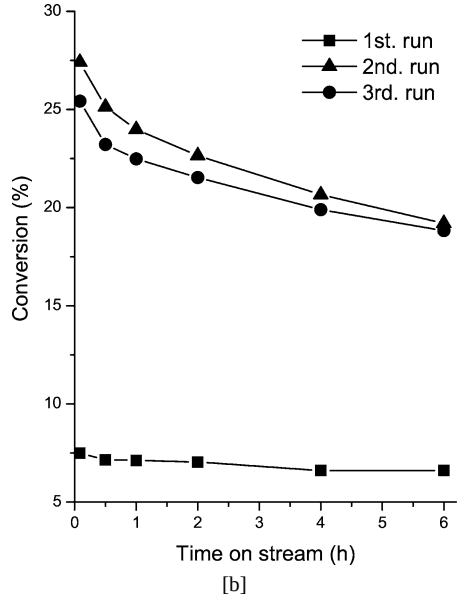

[b]

Fig. 9. [a] Activity profiles of co-precipitated AWZ catalyst for three repeated runs. [b] Activity profiles of co-precipitated PAWZ catalyst for three repeated runs.

was used for the sake of consistency and AWZ catalysts in this series were prepared by an impregnation technique. The performance of WZ catalysts with different Al content is listed in Table 1. One can see that maximum catalytic performance occurs at an Al content of about 0.6 wt%. However, not much difference was observed in isobutane selectivity for these catalysts.

Figs. 9a and 9b show the typical activity profiles of AWZ_C and $PAWZ_C$ catalysts, respectively. Both catalysts were prepared by a co-precipitation technique with 1.0 wt% of Al. They were tested for three repeated catalytic runs and with catalyst regeneration between each run. One can see that the first run (fresh catalysts) always gives the lowest activity, whereas tremendous improvement in activity was observed in the second and third runs (regenerated catalysts). The difference in activity between the last two runs is not great. We have noted that Pt addition not only increases the catalytic activity significantly but also improves the catalytic stability during the course of reaction.

If the catalyst after in situ regeneration was pre-exposed to external atmosphere for 3.5 days before reaction, its catalytic activity decreases significantly as shown in Fig. 10.

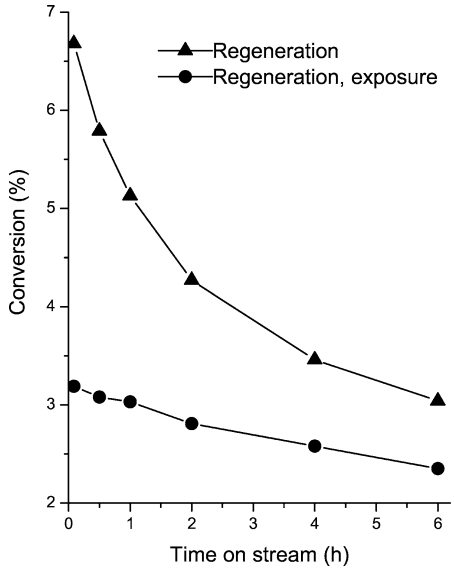

Fig. 10. Effect of pre-exposure to external atmosphere on the catalytic performance of co-precipitated AWZ catalyst after regeneration.

However, the catalytic performance of this catalyst is still better than the fresh catalyst (see Fig. 9a).

The presence of Al in WZ or PWZ catalysts also improves the stability of the catalyst in the course of reaction. Fig. 11 compares the case for fresh PWZ_C and $PAWZ_C$ catalysts. The first-order exponential decay rate constants calculated for PWZ_C and $PAWZ_C$ catalysts are 1.68×10^{-4} and $1.08 \times 10^{-4}\ s^{-1}$, respectively. Comparison for regenerated catalysts is not meaningful due to the large difference in catalytic activity between Al-promoted and nonpromoted catalysts (Table 2). By comparing the regenerated AWZ_C and FWZ_I (or $PAWZ_C$ and $PFWZ_I$) catalysts with comparable activity, one can see that the Al-promoted catalysts also have higher catalytic stability than Fe-promoted catalysts.

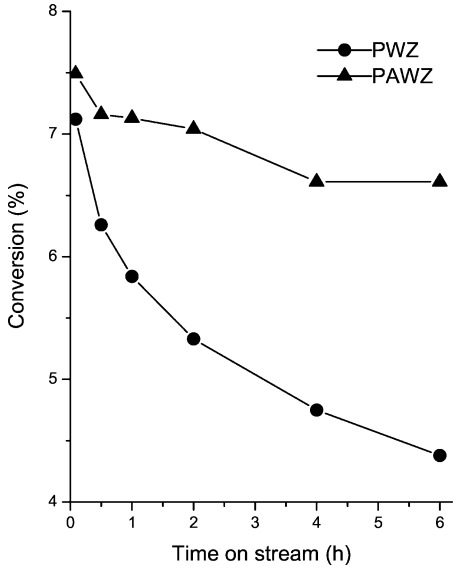

Fig. 11. Effect of Al on the catalytic stability of co-precipitated PWZ catalyst.

Table 2
Catalytic performance of various promoted WZ catalysts in their fresh and regeneration states

Sample	TON[a] ($\mu mol\ g^{-1}\ s^{-1}$)			
	Fresh catalyst		Regenerated catalyst	
	Initial	Final	Initial	Final
WZ_C	0.08	0.03	0.13	0.07
AWZ_C	0.10	0.06	0.59	0.30
FWZ_I	0.20	0.12	0.52	0.20
PWZ_C	0.64	0.39	0.94	0.63
$PAWZ_C$	0.67	0.59	2.45	1.71
$PFWZ_I$	1.53	1.03	2.48	1.48

[a] Initial and final data were obtained after 5 min and 6 h on stream, respectively.

To see more clearly the influence of various promoters and pretreatment conditions on the performance of WZ catalysts, we summarized the important catalytic data in Table 2. Both Al (1.0 wt%) and Fe (1.2 wt%) can improve the catalytic performance of WZ catalysts, either with or without Pt addition. However, the extent of promotion effect exerted by Al and Fe varies in fresh and regenerated catalysts. In fresh catalyst, the initial catalytic performance (after 5 min on stream) decreases in the order $FWZ_I > AWZ_C \geqslant WZ_C$. In regenerated catalysts, however, the order becomes $AWZ_C \geqslant FWZ_I > WZ_C$. Now, AWZ_C is as active as the FWZ_I catalyst. This phenomenon is also observed in Pt-loaded samples.

We have also analyzed the carbon content on our best performance catalysts after catalytic runs. The carbon contents on the used PWZ_C, $PAWZ_C$, and $PFWZ_I$ are 0.03, 0.08, and 0.35 wt%, respectively. The first two catalysts have negligible carbon content but the last one is relatively high. We ought to mention that our used catalysts were cooled from 300 to 200 °C under H_2 flow and the flow was stopped after further cooling.

4. Discussion

4.1. Effect of Al addition on WZ catalyst

Since the discovery of the special catalytic properties of the WZ catalyst system in *n*-alkane isomerization reaction [7], tremendous effort has been devoted to the understanding of the catalytic role played by this catalyst. In this respect, the structural information of WO_x species on ZrO_2 support becomes very important since it helps to reveal the surface chemistry occurring on this catalyst during isomerization reaction. Therefore, the studies on the structural characterization of this type of catalysts have become the focal point of recent research [13,25–27].

The structure of WO_x supported on ZrO_2 has been well characterized by the in situ XANES and EXAFS studies

of Barton et al. [13]. Their W-L_I-edge XANES results of WZ after dehydration at 450 °C suggest that the W centers are located in a distorted octahedral oxygen environment. Besides, both their XANES and EXAFS results showed the resemblance in structural symmetry between WO_x supported on ZrO_2 and bulk WO_3 for all WO_x concentration and pretreatment conditions. Our EXAFS RDF plots of WZ catalysts are similar to those reported by Barton et al. [13] but with better peak resolution. In addition, our DRIFT results also confirmed the reported observation of a W=O functional group on WZ [27]. Taking into account the results from XRD study, it is evidence that WO_x crystallites are present on both co-precipitated and impregnated WZ catalysts and has a tetragonal WO_3-like structure.

Although our XANES study suggests that the addition of Al onto WZ catalysts does not affect the symmetry around W atoms, the structure of the WO_x phase seems altered as shown by the XRD results. The disappearance of WO_x diffraction peaks after Al addition in impregnated AWZ catalysts indicates strong interaction between W and Al species during catalyst preparation. The change in sample color from yellowish (WZ) to white (AWZ) also provides support evident in W–Al interactions. However, the WO_x XRD peaks and sample color in co-precipitated AWZ catalyst are less affected by Al addition. Possibly, the Al species are now well dispersed throughout the bulk of the catalyst and a lesser amount is available for interaction with WO_x. The sharp ^{27}Al MAS NMR resonance signal recorded for co-precipitated catalyst also suggests a better distribution of Al species in the WZ structure than impregnated catalyst.

Since the EXAFS technique is sensitive to the local environments of the W atom absorber, we used it to compare the local structure of the W atom in our WZ and AWZ catalysts. In the impregnated samples, the W–O and W–O–W bonding regions are not affected much after Al addition. Only one W–O–Al linkage appears. It seems that the addition of Al does not have a serious effect on the local structure of WO_x originally present in WZ catalysts. The bonding between WO_x and Al species probably occurs through the condensation of hydroxyl groups, and this leads to the formation of a single W–O–Al corner-sharing link (terminal Al^{3+} sites). The presence of Brönsted OH groups on WO_x has been demonstrated by our DRIFT study. With reference to the case of iron compounds, this type of linkage will give a bond distance of about 4 Å [28]. The absence of WO_x XRD peaks in the impregnated AWZ catalyst means that Al species retard its crystallization process. The lack of contribution from large crystallites of WO_x might explain the white color of the sample. Obviously, excess Al exists as discrete oxides on the AWZ_I surface.

In the RDF plots of co-precipitated AWZ catalyst, we have found various changes in the local structure of WO_x relative to WZ. First, the interaction between W and Al species causes the W–O–W distances to shrink significantly. Then, the W–O bonding region is also modified by Al addition and the bond length becomes more disordered. Most importantly, an additional but shorter W–O–Al linkage is formed besides the original one in impregnated AWZ catalysts. We suspect that this new Al^{3+} site is formed through substitution of Al species into the WO_x structure (substituted Al^{3+} sites). The shorter W–O–Al distance of this substituted Al^{3+} site than the terminal Al^{3+} site is reasonable since the former is constrained by WO_x structure. It seems that this substituted Al^{3+} site has less effect on the color of WZ than the terminal Al^{3+} site.

Other than the W–O–W/Zr peak, our catalysts did not give any new peak that can be assigned to W–O–Zr linkage. This finding might indicate that the W–O–Zr bonds are very uniform in length and nature, and this is in line with the well-known monolayer formation of WO_x on ZrO_2 support. The formation of this bond is likely due to the condensation of W–OH and Zr–OH groups. In addition, previous study has shown that the surface Zr–OH groups disappeared as the WO_3 loading approached saturation [9].

4.2. Catalytic performance of WZ and AWZ catalysts

There are three important findings in our catalytic studies. First, Al was found to act as a promoter for WZ catalysts in *n*-butane isomerization reaction (Tables 1 and 2). Second, a great leap in catalytic activity was observed for regenerated catalyst relative to fresh catalyst (Figs. 9a and 9b). Finally, the added Al improves the catalytic stability of WZ catalyst during the reaction (Fig. 11).

In the impregnated AWZ catalysts, one can see that the promotion effect of Al is most effective at loading less than 1 wt% (Table 1). Possibly, Al loading beyond this value will form a considerable amount of oxide species on the catalyst surface and then cause physical blocking of active sites for the isomerization reaction. This might be the origin of the broad resonance in ^{27}Al MAS NMR spectra assigned to disordered Al species. However, we cannot exclude the geometric effect where the adjacent adsorption sites required for the formation of C_8 intermediate are disrupted by these Al species.

We have also compared the catalytic performance of Al- and Fe-promoted catalysts. In fresh catalysts, the catalytic performance decreases in the order $FWZ_I > AWZ_C \geqslant WZ_C$. Here, the activity of AWZ_C is comparable to that of WZ_C. This trend is reasonable since Fe is well-known to act as promoter in an alkane isomerization reaction in both SZ and WZ systems [10,29]. In regenerated catalysts, the catalytic performance follows the order $AWZ_C \geqslant FWZ_I > WZ_C$. We can now see that AWZ_C is much more active than WZ_C catalyst. Al is even as active as Fe in promoting an alkane isomerization reaction in our catalytic system. We explain the promotion effect of Al in terms of the increased amount of acid sites in AWZ_C over WZ_C catalysts. Our NH_3-TPD results revealed that the additional amount of acid sites created by Al is at least moderate in strength. In addition, our DRIFT results seem to indicate that these

newly created acid sites (L_{LN}) have higher acid strength than the Brönsted and Lewis acid sites originally present in WZ. In the study on persulfated Al-promoted zirconia catalysts by Xia et al. [4], they have also shown that Al addition caused an enhancement in the number of acid sites with intermediate acid strengths. Interestingly, our reference catalyst (FWZ_I) has lower total acidity but higher catalytic activity than WZ_C catalyst. This phenomenon leads us to assume a nonacidic promotion behavior of Fe in alkane isomerization reaction.

The jump in activity from fresh to regenerated catalyst is particularly interesting and prominent for Al-containing WZ catalysts. The reason for the great leap in catalytic activity is not yet fully understood. It is not due to coke residue on regenerated catalyst since coke has a negative effect on the reaction activity. We believed that this peculiar behaviour is associated with the residual amount of water chemisorbed on the catalyst surface. In other words, the function of Al and Fe promoters will be affected by chemisorbed water. The temperature used for catalyst regeneration (450 °C) is higher than the pretreatment (dehydration) and reaction temperatures (300 °C) used for the fresh catalysts; hence, less water is present in the regenerated catalysts. This explains the jump in catalytic activity from fresh to regenerated catalysts since more promoter sites will be exposed in the latter for catalytic reaction. We have further tested a fresh catalyst with a higher pretreatment temperature of 450 °C (6 h) and indeed found no such activity jump since its activity equals the regenerated one. This result also confirms that the effect of residual carbon (if any) on the regenerated catalysts is minimal. It is also not surprising to find that the activity of this fresh catalyst is higher than that of the fresh catalyst pretreated at 300 °C.

To further check this suggestion, we carried out dehydration studies on WZ_C, AWZ_C, and FWZ_I catalysts, and the water content in their fresh and regenerated states is compared. Generally, we found that all these catalysts have less chemisorbed water in the regenerated state than in their corresponding fresh state. The difference in water content is 0.21, 0.22, and 0.13 wt% for WZ_C, AWZ_C, and FWZ_I catalysts, respectively. These data support our proposal given above. Specifically, regenerating the AWZ_C catalyst will expose a larger fraction of promoter than FWZ_I due to a greater amount of water loss, which then takes part in the reaction. Hence, the activity jump is higher in AWZ_C than in FWZ_I catalysts. We have noted that WZ_C has a comparable amount of water loss to AWZ_C catalyst. However, since it has no promoter to exert the effect of dehydration, the jump in catalytic activity is the least.

The effect of surface chemisorbed water on catalytic performance has also been observed in SZ systems [30]. It has been shown that an optimum pretreatment temperature (300–400 °C) exists that will produce the highest catalytic activity. Therefore, the performance of catalyst can change according to the degree of hydration of its surface by varying the amount of accessible active sites for the reaction. However, their regenerated catalysts (500 °C in O_2 for 1 h) require a rehydration step to regain its original catalytic activity, although not completely. The authors explained their finding by assuming that rehydration restores the original ratio of Brönsted to Lewis acid sites on the catalyst surface. These results are unlike our AWZ_C catalysts where regenerated catalyst is much more active than fresh catalyst. Besides, rehydration of our catalyst by exposure to the atmosphere has a negative effect on catalytic performance (Fig. 10). We suspect that different type(s) of acid sites is/are operational here in AWZ_C catalysts. In the next section, we shall try to identify the nature of acid sites responsible for the catalytic activity of AWZ_C catalysts.

Until now, we do not yet have a clear understanding on the stabilization effect of Al on the catalytic performance of AWZ_C and $PAWZ_C$ catalysts. The role of Al in this respect may be complex and it might act through a combination of pathways. Anyway, we think that the inert nature of Al in the reducing environment of the reactant might be the prime factor. In $PAWZ_C$ catalyst, Al probably improves the stability of Pt through an ensemble effect and thus minimizing the sintering and carbide formation processes. Interestingly, both the used PWZ_C and $PAWZ_C$ catalysts seem to have negligible coke formation.

4.3. Nature and behaviour of acid sites in AWZ catalysts

Transition metals like Pt are widely known as promoters in acid-catalyzed *n*-butane isomerization reactions [13,14]. Therefore, the nature of the promotion effect of Pt will not be discussed here. Pt can generate Brönsted acidity in the presence of H_2 and thus is capable of increasing and stabilizing the catalytic activity. Although Al is not a transition metal, our results and those from SZ have shown conclusively that it can act through the formation of a new type of acid sites on the catalyst. In our study, we have found that Al addition creates an additional type of Lewis acid sites (L_{LN}) on AWZ catalyst, which may be responsible for the three interesting phenomena observed in *n*-butane isomerization reactions. In other words, the acidic L_{LN} sites are the promoter sites in AWZ catalysts.

Considering all the catalyst characterization and catalytic results, we put forward a simplified account to describe the behaviour of AWZ catalyst in the *n*-butane isomerization process:

(i) During the catalyst preparation processes at 800 °C, some Al species react with WO_x, leading to the formation of substituted and terminal Al^{3+} sites. These sites constitute the L_{LN} sites. When the sample was cooled to room temperature and came into contact with atmospheric water, these L_{LN} sites will be poisoned by chemisorbed water. The number of water molecules adsorbed on each L_{LN} site may vary so that an octahedral symmetry around Al can be built. The octahedral symmetry of these sites has been shown by ^{27}Al MAS NMR study.

(ii) In the first catalytic run with fresh AWZ catalyst, the pretreatment temperature used is 300 °C and this is not enough to fully remove the chemisorbed water on L_{LN} sites. Hence, the promotion effect of Al in catalytic reaction for fresh catalyst is not strong.

(iii) Upon regeneration of the used catalyst at 450 °C, the L_{LN} sites are now fully recovered. Besides the increased amount of L_{LN} sites, the acid strength of these sites also increases since this catalyst has been subjected to a higher temperature. Thus, a great leap in the catalytic activity of regenerated catalyst relative to fresh catalyst can be envisaged.

5. Conclusion

Besides the more commonly used promoters like Pt and Fe, we have found a non-transition-metal like Al as the promoter for WZ in the *n*-butane isomerization reaction. In our study, we have demonstrated that the activity of WZ catalyst in the reaction can be improved by the addition of Al. The performance of AWZ_C catalyst equals that of FWZ_I but not PWZ_C, which means that the role of Pt in the reaction is still unsurpassed. We have shown that doubly promoted $PAWZ_C$ catalyst exhibits the highest catalytic activity and stability in the reaction.

The nature of Al promotional effect is probably through the formation of a new type of Lewis acid sites with at least moderate acid strength. The acid strength of these L_{LN} sites is stronger than the Brönsted and Lewis acid sites originally present on WZ catalyst. Higher pretreatment (or regeneration) temperatures favor the promotion effect of Al by decreasing the amount of surface chemisorbed water that poisons the L_{LN} sites. Besides, their acid strength also increases with temperature. Both these factors contribute to the great improvement in catalytic activity of AWZ catalyst relative to WZ catalyst after regeneration.

Therefore, the promotion effect of Al is very different from that of Fe. The difference in the order of performance for AWZ_C and FWZ_I catalysts in the fresh and regenerated states is also in line with this proposition. So far, Fe is not known to act through acidity effect like Al. Al also has an added advantage of stability in the reaction. Unlike Fe, the nature of Al should not be much affected under the reducing environment of the reactant. This could explain the higher catalytic stability of AWZ_C than FWZ_I in the *n*-butane isomerization reaction. The surprisingly high content of carbon on the used $PFWZ_I$ catalyst is probably due largely to the formation of iron carbide.

Besides the acidity effect, the addition of Al can also affect the crystallite size of WO_x on WZ. In this paper, we have not discussed the effect of crystallite size of WO_x on the catalytic performance. Further study on this should be interesting.

Acknowledgments

We are grateful for the financial support of China Petroleum Co. and the National Science Council of Taiwan. We would like to thank MEL for the gift of free tungstated zirconia precursors. We also want to extent our gratitude to Dr. Q. Zhao of Academia Sinica for NMR measurements, and Dr. T.C. Tsai from CPC for helpful discussion.

References

[1] I.E. Maxwell, J.E. Naber, Catal. Lett. 12 (1992) 105.
[2] A. Corma, A. Martínez, Catal. Rev.-Sci. Eng. 35 (1993) 483.
[3] K. Tanabe, H. Hattori, Chem. Lett. (1976) 625.
[4] Y. Xia, W. Hua, Z. Gao, Appl. Catal. 185 (1999) 293.
[5] C.L. Chen, S. Cheng, H.P. Lin, S.T. Wong, C.Y. Mou, Appl. Catal. 215 (2001) 21.
[6] C.L. Chen, T. Li, S. Cheng, N.P. Xu, C.Y. Mou, Catal. Lett. 78 (2002) 223.
[7] M. Hino, K. Arata, J. Chem. Soc. Chem. Commun. (1988) 1259.
[8] J.C. Yori, C.L. Pieck, J.M. Parera, Appl. Catal. 181 (1999) 5.
[9] M. Scheithauer, T.K. Cheung, R.E. Jentoft, R.K. Grasselli, B.C. Gates, H. Knözinger, J. Catal. 180 (1998) 1.
[10] J.C. Vartuli, J.G. Santiesteban, P. Traverso, N. Cardona-Martinéz, C.D. Chang, S.A. Stevenson, J. Catal. 187 (1999) 131.
[11] S.R. Vaudagna, S.A. Canavese, R.A. Comelli, N.S. Fígoli, Appl. Catal. 168 (1998) 93.
[12] S.R. Vaudagna, R.A. Comelli, N.S. Fígoli, Appl. Catal. 164 (1997) 265.
[13] D.G. Barton, S.L. Soled, G.D. Meitzner, G.A. Fuentes, E. Iglesia, J. Catal. 181 (1999) 57.
[14] X. Song, A. Sayari, Catal. Rev.-Sci. Eng. 38 (1996) 329.
[15] M.R. Guisnet, Acc. Chem. Res. 23 (1990) 392.
[16] N. Naito, N. Katada, M. Niwa, J. Phys. Chem. B 103 (1999) 7206.
[17] S. Kuba, P.C. Heydorn, R.K. Grasselli, B.C. Gates, M. Che, H. Knözinger, Phys. Chem. Chem. Phys. 3 (2001) 146.
[18] P. Kubelka, F. Munk, Z. Technol. Phys. 12 (1931) 593.
[19] J.H. Choy, J.B. Yoon, D.K. Kim, S.H. Hwang, Inorg. Chem. 34 (1995) 6524.
[20] M.A. Coelho, D.E. Resasco, E.C. Sikabwe, R.L. White, Catal. Lett. 32 (1995) 253.
[21] G. Larsen, E. Lotero, S. Raghavan, R.D. Parra, C.A. Querini, Appl. Catal. 139 (1996) 201.
[22] C. Bigey, L. Hilaire, G. Maire, J. Catal. 184 (1999) 406.
[23] R.A. Boyse, E.I. Ko, Appl. Catal. 177 (1999) L131.
[24] C.D. Baertsch, S.L. Soled, E. Iglesia, J. Phys. Chem. B 105 (2001) 1320.
[25] F. Hilbrig, H.E. Göbel, H. Knözinger, H. Schmelz, B. Lengeler, J. Phys. Chem. B 95 (1991) 6973.
[26] A. Burrows, C.J. Kiely, R.W. Joyner, H.K. Knözinger, F. Lange, Catal. Lett. 39 (1996) 219.
[27] D.S. Kim, M. Ostromecki, I.E. Wachs, J. Mol. Catal. 106 (1996) 93.
[28] J. Rose, A. Manceau, J.Y. Bottero, A. Masion, F. Garcia, Langmuir 12 (1996) 6701.
[29] F.C. Lange, T.K. Cheung, B.C. Gates, Catal. Lett. 41 (1996) 95.
[30] M. Risch, E.E. Wolf, Appl. Catal. 206 (2001) 283.